

Parasitic filtering in position detection systems for optical tweezers

Kirstine Berg-Sørensen^a, Erwin J. G. Peterman^b, Lene Oddershede^a, Meindert van Dijk^b, Ernst-Ludwig Florin^c, Christoph F. Schmidt^b, and Henrik Flyvbjerg^d

^aNiels Bohr Institute, Blegdamsvej 17, Copenhagen, Denmark;

^bDepartment of Physics and Astronomy, Faculty of Sciences, Vrije Universiteit, De Boelelaan 1081, 1081 HV, Amsterdam, The Netherlands;

^cPhysics Department and Center for Nonlinear Dynamics, The University of Texas at Austin, 1 University Station C1600, Austin, TX78712, USA;

^dPlant Research Dept. and Danish Polymer Centre, Risø National Lab., Roskilde, Denmark

ABSTRACT

In a typical position detection system for optical tweezers, laser light impinges on a quadrant photodiode, and the signal from the four quadrants of the diode is used to determine the position of a trapped object. A widely used position detection system consists of a Si-PIN photodiode and an infrared laser. In previous work we have demonstrated with two distinct experimental methods how such a system may act as an unintended low-pass filter and we modeled its physical origin mathematically. Here we demonstrate that the general solution to this model can account precisely for the “parasitic” filter’s effects up to as large frequencies as we can measure, approximately 100 kHz. Thus we increase the useful bandwidth of tweezers experiments by nearly two decades. This opens for investigations of phenomena in biophysics, soft matter, and polymer science at much higher frequencies than before.

Keywords: Optical tweezers, photodiode detection, power spectrum analysis

1. INTRODUCTION AND BACKGROUND

Photodiodes are used for detection of position in a number of modern techniques; for example in atomic force microscopy^{1,2} and optical tweezers.^{3,4} We here concentrate on optical tweezers, with position detection by a Si-PIN photodiode, illuminated by the trapping laser light. In previous work we have demonstrated that delayed detection of most charge carriers created by photon absorption in the diode, gives rise to an output signal that relates to the input of light as if the signal had been low-pass filtered.^{5,6} We also demonstrated that this effect depends on the laser’s wavelength as it should, according to the physical explanation of the phenomenon.^{7,8} In the power spectrum of the position signal, the effect is seen as a loss of power, visible already at 1 kHz⁶ and exceeding 50% above, typically, 7–10 kHz for an infrared laser and a Si-PIN diode,^{6,9,10} i.e., it is seen as if the system contains an unintended low-pass filter, a “parasitic” filter.

Here, we review how a simple physical model of the dynamics of photo-detection in the Si-PIN photodiode can account accurately for this parasitic filter’s effect on experimental results. We present some new results on this, showing how the model is solved and the solution utilized up to much higher power spectral frequencies than hitherto. We also show that the model works equally well for a different kind of photodiode.

This development of optical tweezers to a tool of high precision and high bandwidth has already paid off in studies of two biological systems,^{11–13} and the additional tripling of the bandwidth discussed here opens up for more possibilities in the same vein and other fields, like rheology and polymer science.

The paper is organized as follows: Section 2 describes our simple physical model of the dynamics of photo detection in the photodiode. Sections 3 and 4 present and analyze the two experiments. Section 5 concludes.

Further author information: Corresponding author: Kirstine Berg-Sørensen, E-mail: berg@nbi.dk

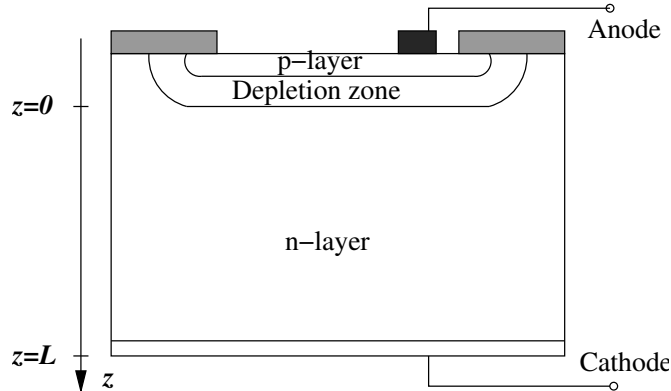


Figure 1. Typical cross-section of a photodiode. Reproduced from Ref. 16. Not to scale. Typical dimensions are L of order a few hundred μm and thickness of p-layer and depletion zone of a few to tens of a μm .

2. HOW TO COPE WITH TRANSPARENT PHOTO DETECTORS

The photo-active area of a Si-PIN photodiode is layered: it consists of a thin layer of p -doped Si (p -layer) through which the light enters, a depletion zone that is the intended photo detection zone, and a thicker substrate layer, typically of n -doped Si. The difference in charge density in the p - and n -layers results in an electrical field across the depletion zone.¹⁴ Pairs of charge-carriers that are created by photons absorbed in the depletion zone, are swiftly swept away by this field and detected within nanoseconds of their creation as a current that is the intended output signal of the photodiode.¹⁵ Silicon is somewhat transparent to infrared light, however. So some infrared photons pass straight through the depletion zone, and some of these are absorbed in the n -layer, which is thicker, hence produce more charge carriers at high transparency. These charge-carriers find themselves in a field-free region, and only gradually diffuse into the depletion zone, where they are detected with corresponding delays.

The output of the photodiode detection system can be modeled as a sum of two parts: (i) an (effectively) instantaneous part from the fraction of photons absorbed in the depletion zone, and (ii) a delayed part from the photons absorbed in the n -layer.⁵ In the simplest version of our physical model, we describe the diode's geometry with two parameters, the thickness $L^{(\text{dep})}$ of the depletion zone and the thickness L of the n -layer. We denote the coordinate along the light's path through the diode by z , see Fig. 1, with $z = 0$ corresponding to the interface between the depletion zone and the n -layer, and $z = L$ corresponding to the position of the cathode. The laser light's absorption coefficient we denote by a . The delayed signal is predominantly caused by holes in the n -layer,⁵ so we consider only positive charge-carriers.

The density of charge-carriers created by an infinitely brief flash of light at time $t = 0$ is, at $t = 0$, $\rho(z, t) = \rho_0 \exp(-az)$. In the n -layer, the time-evolution of this distribution is governed by the diffusion equation with appropriate boundary conditions. Its values at later times can be written as a superposition of eigenfunctions $h_n(z)$ with appropriate boundary condition for the operator describing diffusion, i.e., the Laplacian in the field-free case, and in general the Laplacian plus a convective term,

$$\rho(z, t) = \rho_0 \sum_{n=0}^{\infty} b_n \exp(-t/\tau_n) h_n(z) . \quad (1)$$

In the simplest version of the model, we assume a completely field-free n -layer. The boundary conditions are absorbing at $z = 0$ and reflecting at $z = L$, and the eigenfunctions are easily found, $h_n(z) = \sin(\frac{(2n+1)\pi}{2} \frac{z}{L})$. In that case, all coefficients b_n are known as functions of a , L , and the index n , see Eq. (11) in Ref. 8. The characteristic delay times τ_n in this case are

$$\tau_n = D^{-1} \left(\frac{2L}{(2n+1)\pi} \right)^2 . \quad (2)$$

In the most general case, the coefficients b_n are only related by normalization, but because the n -layer is a compact volume, the spectrum of relaxation times τ_n remains discrete. Thus, in practice a finite number of terms, $N + 1$, exhausts the sum.

In general, the temporal response of the photodiode can, in practice, be described with the response function

$$g(t) = \alpha^{(\text{diode}, N)} \delta(t) + (1 - \alpha^{(\text{diode}, N)}) C_N \sum_{n=0}^N (2n + 1) b_n \exp\left(-\frac{t}{\tau_n}\right). \quad (3)$$

It describes the output at time t in response to a flash of light at time $t = 0$. Here, $1 - \alpha^{(\text{diode}, N)}$ is the fraction of the signal contained in the slowest $N + 1$ relaxation modes of the diffusion equation, and $\alpha^{(\text{diode}, N)}$ is the fraction of the signal contained in the faster modes, assuming that these are so fast that they appear as instantaneous in the approximation we work in. The fastest relaxation mode N to include explicitly in Eq. (3) is determined by the smallest time interval one's data can resolve, i.e., by the data acquisition rate, or, equivalently, the Nyquist frequency of the signal's power spectrum.

Thus, where an infinitely fast detection system would produce an output signal $S(t)$, our system produces a delayed output $S^{(\text{del})}(t)$,

$$S^{(\text{del})}(t) = \int_{-\infty}^t g(t - t') S(t') dt' . \quad (4)$$

In Fourier space, by virtue of the convolution theorem, Eq. (4) reads

$$\tilde{S}^{(\text{del})}(f) = \tilde{S}(f) \cdot \tilde{g}(f) , \quad (5)$$

where $\tilde{}$ denotes Fourier transformation. Thus, the recorded, experimental power spectrum $P^{(\text{ex})}(f) \equiv \langle |\tilde{S}^{(\text{del})}(f)|^2 \rangle$ is simply the power spectrum of the physical signal $\langle |\tilde{S}(f)|^2 \rangle$ multiplied by $G(f) \equiv |\tilde{g}(f)|^2$. From Eq. (3) we find⁸

$$G(f) = (\alpha^{(\text{diode}, N)})^2 + (1 - \alpha^{(\text{diode}, N)})^2 C_N^2 \left\{ \sum_{n=0}^N \frac{(\zeta_n)^2}{1 + (f/f_n)^2} + \sum_{n=0}^N \sum_{n' < n} \frac{\zeta_n \zeta_{n'} (1 + (f/f_n)(f/f_{n'}))}{(1 + (f/f_n)^2)(1 + (f/f_{n'})^2)} \right\} \\ + 2\alpha^{(\text{diode}, N)} (1 - \alpha^{(\text{diode}, N)}) C_N \sum_{n=0}^N \frac{\zeta_n}{1 + (f/f_n)^2} \quad (6)$$

with $\zeta_n = (2n + 1)b_n\tau_n$, $C_N = (\sum_{n=0}^N \zeta_n)^{-1}$ and $f_n \equiv 1/(2\pi\tau_n)$. With $N = 0$, we obtain the simplest response,

$$G_0(f) = \alpha^{(\text{diode})^2} + \frac{1 - \alpha^{(\text{diode})^2}}{1 + (f/f_{3\text{dB}}^{(\text{diode})})^2} \quad (7)$$

with $f_{3\text{dB}}^{(\text{diode})} \equiv f_0$. This simple function simplifies further to a first-order filter characteristics containing only one parameter, a combination of $\alpha^{(\text{diode})^2}$ and $f_{3\text{dB}}^{(\text{diode})}$, in an approximation valid for laser wavelengths in the near infrared (~ 1000 nm) where $\alpha^{(\text{diode})^2}$ is small, provided the maximum frequency considered is less than ~ 10 kHz, so $(f/f_{3\text{dB}}^{(\text{diode})})^2 < 1$.^{5, 6}

In the two subsequent sections, two very different types of experiments are described. Both verify the model outlined above, and the second exploits it to its limits.

3. EXPERIMENT WITH CHOPPED LASER BEAM

A very simple experiment shows directly that the photodiode detection system acts as a filter⁵: The laser beam is focused and impinges directly on the quadrant photodiode. This beam is chopped mechanically with frequency f_{chop} . By varying this frequency while keeping the laser intensity constant, we can measure the characteristic function $G(f)$ fairly directly.

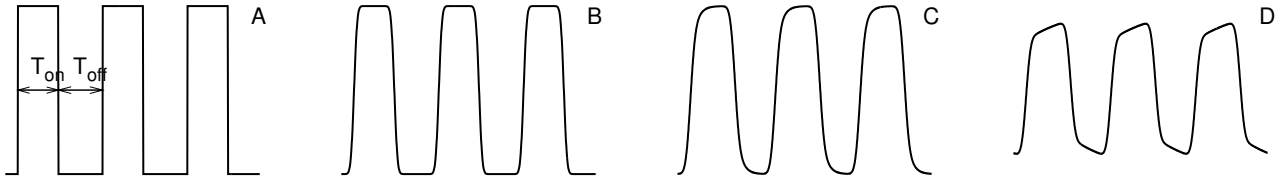


Figure 2. Sketch of the model for the output produced by a chopped Gaussian infrared laser beam impinging on a silicon diode. A: Train of rectangular output pulses that result from chopping an infinitely thin beam of light, followed by detection with no delay. The ratio between on-time and off-time, $T_{\text{on}}/T_{\text{off}}$, is given by the geometry of the chopper wheel. B: Train of output pulses that result from chopping a Gaussian beam profile, followed by detection with no delay. C: Same as B, but output pulses were filtered by a first-order filter, hence delayed with a simple exponential response function $g(t) = \exp(t/\tau)/\tau$ with $\tau \ll T_{\text{off}}, T_{\text{on}}$. D: Same as C, but with $\tau \approx T_{\text{off}}, T_{\text{on}}$.

The experiment is analyzed as follows: The laser beam has a Gaussian intensity profile. Thus, instead of a train of rectangular pulses (Fig. 2A), the light hitting the diode varies in intensity like a train of pulses with transients shaped like error-functions (Fig. 2B). This input produces a delayed output, cf. Eq. (4), which is seen more clearly, the larger the delay time τ_0 of Eq. (2) is, compared to the time $\sigma_t \propto 1/f_{\text{chop}}$ that it takes for the edge of a hole in the mechanical chopper to sweep across the Gaussian beam profile. A case where τ_0 is equal to σ_t is illustrated in Fig. 2C, and one where τ_0 is an order of magnitude larger than σ_t is shown in Fig. 2D.

The analysis of the chopped signal in the time-domain is explained in detail in Ref. 5. In that paper, chopping frequencies between a few hundred Hz and 14 kHz were analyzed. The characteristic delay time τ_0 was slightly longer than the shortest sweep-time σ_t . For the lowest chopping frequencies, the recorded signal resembles the train of pulses shown in Fig. 2B and the delay is not visible. For intermediate chopping frequencies, the pulse-shape resembles that shown in Fig. 2C. For the highest values of f_{chop} , the shape of the signal is dominated by the delay, cf. Fig. 2D. Thus, in this very simple experiment already from the unprocessed signal in the time domain one sees the relevant time-scales of the problem.

The experimental characteristic function $G^{(\text{ex})}(f)$ is found as follows: For a periodic input signal $S(t)$, the output signal is necessarily periodic with the same period. So its power spectrum vanishes except at frequencies $f_k = kf_{\text{chop}}$, where k is an integer. In the ideal case of a perfectly periodic input signal recorded for infinite time, the power spectrum of the output takes the form

$$P(f) = \sum_k P_k \delta(f - f_k) . \quad (8)$$

Our chopper is not perfectly periodic because its holes are not perfectly identical and equidistant. Consequently, the delta-functions in Eq. (8) are seen as peaks of finite width in the power spectrum. Also, we measure for finite time, which causes *leakage*,¹⁷ another, specific kind of significant broadening of peaks, which we reduce significantly by so-called *windowing*,¹⁷ using a Hann window. These technical details matter for the practical implementation of the mathematical result we use, but do not affect the result itself, which states⁵ that the integral power in any one of the peaks represented by delta-functions in Eq. (8) is reduced by a factor $G(f_{\text{chop}})$ compared to its integral power in the limit $f_{\text{chop}} \rightarrow 0$. Thus, simply by measuring the power in a peak as function of f_{chop} , one has measured $G(f)$. Our result of such measurements is shown in Fig. 3, fitted with the response function $G_0(f)$ of Eq. (7). The laser-intensity-dependence of $f_{3\text{dB}}^{(\text{diode})}$ is maybe caused by a small dependence in the width of the depletion layer on the number of charge-carriers excited in the n -layer.

Since the parasitic filter's characteristic function depends on the intensity of the laser light falling on the diode, it varies from one experiment to the next. Consequently, parasitic filtering should be accounted for as an integral part of the calibration of optical tweezers. Several examples of how this is done are found in Refs. 6, 11–13. Below, we describe one of these examples.

4. EXPERIMENTS WITH TRAPPED SILICA BEADS

The chopper experiment of the previous section can only probe $G(f)$ up to the maximum frequency that the chopper wheel can deliver, or, if based on a peak at kf_{chop} , to k times this maximum frequency. As the integral

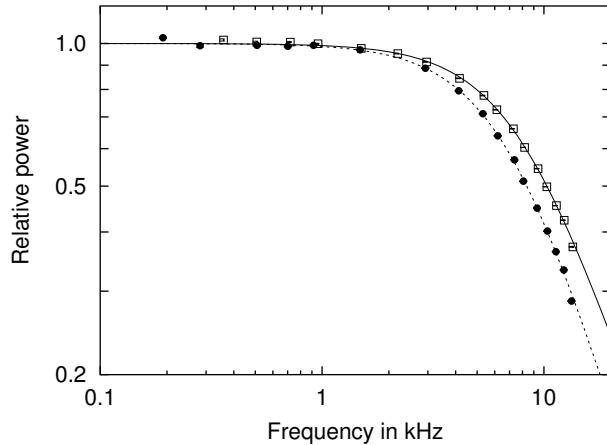


Figure 3. The characteristic function of the photodiode, as measured in an experiment with a chopped laser beam of wavelength 1064 nm.⁵ Results shown as open squares were obtained with laser intensity roughly 4 times larger than the intensity used to obtain results shown as filled circles. The solid and dashed lines are fits of Eq. (7) to the data, yielding $f_{3\text{dB}}^{(\text{diode})} = 9.3 \pm 0.2$ kHz and $f_{3\text{dB}}^{(\text{diode})} = 7.9 \pm 0.2$ kHz, respectively. The corresponding values for $\alpha^{(\text{diode})}$ are 0.4 ± 0.1 and 0.3 ± 0.1 , respectively.

power in the higher harmonic peaks rapidly decrease with increasing k , this is not a feasible manner in which to reach higher frequencies.

In Ref. 7, Brownian motion was used to produce a known and understood signal sampled at 195 kHz, a limit set by the data acquisition electronics, and not by the Si-PIN photo diode used. Using a tuneable laser, it was demonstrated that the amount of parasitic filtering that occurs, depends on the laser wavelength, as one would expect from the wavelength dependence of silicon’s absorption coefficient. Parasitic filtering gradually disappears as the wavelength is reduced.

In Ref. 8, this wavelength dependence was studied quantitatively, and the characteristic function of the parasitic filter was determined out to 80 kHz. The last 17.5 kHz of the power spectrum out to the Nyquist frequency $195 \text{ kHz}/2 = 97.5 \text{ kHz}$ were excluded because an electronic filter in the data acquisition system cuts off the spectrum already near 90 kHz, with some ripples just below that frequency. Silica beads with a radius of $R = 450 \text{ nm}$ were trapped in optical tweezers formed by either a tuneable Ti:Sapphire laser in the wavelength range 800–1000 nm or by a 1064 nm Nd:YVO₄ laser. Time-series of the position of a trapped bead were detected by back-focal plane interferometry by a Si-PIN photodiode.^{4,18} We also performed experiments where the Si-PIN photodiode was replaced by an InGaAs PIN photodiode (G6849, Hamamatsu, Hersching, Germany).

The position of the trapped bead was measured at a sampling rate of 195 kHz. Analog-to-Digital-Conversion of position measurements was done with $\Delta - \Sigma$ electronics, which apply over-sampling of the signal by a large factor. Thereby, effects of aliasing at the nominal Nyquist frequency are eliminated. The time-series of positions were Fourier transformed, and position power spectra $P^{(\text{ex})}(f)$ were calculated. Such power spectra are often modeled with a Lorentzian,

$$P_{\text{Lorentz}}(f) = \frac{D/(2\pi^2)}{f_c^2 + f^2} \quad (9)$$

which is what the Einstein-Ornstein-Uhlenbeck theory¹⁹ for Brownian motion yields in a low-frequency approximation that neglects the inertial mass of the bead. The Einstein-Ornstein-Uhlenbeck theory is, however, itself a low-frequency approximation to Brownian motion in a liquid because it treats friction as frequency independent and neglects the inertial mass of entrained liquid. It also approximates the thermal noise with white noise, while it really is colored, i.e., has frequency dependent amplitude.¹⁹ The physically correct power spectrum is given in Ref. 6. When the frequency dependent hydrodynamical interaction between the microsphere and the microscope

Table 1. Fitting parameters for the data sets shown in Fig. 4. The frequencies f_0 and f_1 are the characteristic frequencies of the slowest and next-to-slowest eigenmode of diffusion.

System	f_0 (kHz)	f_1 (kHz)	$\alpha^{(\text{diode})2}$
950 nm, Si-PIN diode	14.6 ± 0.2	58.4 ± 0.1	0.45 ± 0.01
1064 nm, InGaAs diode	77 ± 36	-	0.95 ± 0.03

cover-glass surface is also accounted for,^{6, 20} the experimental spectrum is modeled by,^{6, 21}

$$P_{\text{hydro}}(f; R/\ell) = \frac{D/(2\pi^2) \frac{\text{Re } \gamma}{\gamma_0}}{\left(f_c + f \frac{\text{Im } \gamma}{\gamma_0} - f^2/f_m\right)^2 + \left(f \frac{\text{Re } \gamma}{\gamma_0}\right)^2} \quad (10)$$

where

$$\text{Re } \gamma/\gamma_0 = 1 + \sqrt{f/f_\nu} - \frac{3R}{16\ell} + \frac{3R}{4\ell} \exp\left(-\frac{2\ell}{R} \sqrt{f/f_\nu}\right) \cos\left(\frac{2\ell}{R} \sqrt{f/f_\nu}\right) \quad (11)$$

and

$$\text{Im } \gamma/\gamma_0 = -\sqrt{f/f_\nu} + \frac{3R}{4\ell} \exp\left(-\frac{2\ell}{R} \sqrt{f/f_\nu}\right) \sin\left(\frac{2\ell}{R} \sqrt{f/f_\nu}\right). \quad (12)$$

In these expressions, $\gamma_0 = 6\pi\rho\nu R$ is Stokes' friction coefficient with R the radius of the bead and $\rho\nu$ the dynamical viscosity of water. The *corner frequency* $f_c \equiv \kappa/(2\pi\gamma_0)$ has been introduced, and Einstein's relation $D = k_B T/\gamma_0$ between diffusion constant, Boltzmann energy, and friction coefficient, has been used. Two new characteristic frequencies have been introduced: f_ν is the frequency at which oscillations of the bead penetrate a distance equal to the radius of the bead into the liquid, $f_\nu \equiv \nu/(\pi R^2) = 1.6$ MHz. Another characteristic frequency, f_m , appears in the inertial term, $f_m \equiv \gamma_0/(2\pi m) = 1.6$ MHz. These numerical values are for silica beads of $R=450$ nm in water, and their identity up to two leading digits is coincidental. Note that this complicated theory for the power spectrum contains no more free parameters than the simple Lorentzian does, D and f_c .

Power spectra found from time-series recorded with the Si-PIN photodiode were fitted by $G(f)P_{\text{hydro}}(f)$ in the frequency range [105 Hz, 80 kHz]. For wavelengths below ~ 925 nm, only the slowest eigenmode of diffusion was needed to describe the characteristic function of the parasitic filter, i.e., $G(f) = G_0(f)$ of Eq. (7). For larger wavelengths, the two slowest eigenmodes of diffusion in Eq. (6), i.e., $N = 1$, could explain experimental observations.⁸

The parameters in our theory for $G(f)$ were thus determined experimentally. They can also be calculated theoretically from known absorption characteristics of Si. We compared the two and found good agreement.⁸

In Fig. 4, the analysis of two data series is shown. One data set is recorded by the Si-PIN photodiode, with a trapping laser of wavelength of 950 nm, the other data set is recorded by the InGaAs photodiode, for a trapping laser of wavelength 1064 nm. In the former case, we needed two eigenmodes of diffusion in the description of the filtering by the diode, whereas in the latter, one eigenmode was sufficient to describe the data to perfection. The differences between the two cases are reflected in the values of the fitting parameters, given in Table 1: With the Si-PIN photodiode, roughly 45% of the light is detected in the n -layer, and the characteristic frequencies, f_0 and f_1 , of the parasitic filter are well determined. In the InGaAs photodiode, which is engineered to detect infrared light, only 5% of the power spectral signal undergoes filtering, (1064 nm, InGaAs), and the characteristic frequency f_0 is determined with large error. In that case, the covariance between $\alpha^{(\text{diode})2}$ and f_0 is also quite large, -0.97, and one should not over-interpret the significance of the values of the fitted parameters.

It is, however, difficult to judge whether the values of the parameters that we obtain in this manner, are consistent with the physical characteristics of the material of the diode: The information available about the InGaAs diode states that it is of PIN type, like the Si-PIN photodiode, but the material composition (the value of x in $\text{In}_x\text{Ga}_{1-x}\text{As}$) is unavailable and we know neither the diffusion coefficient of charge-carriers in the n -layer, nor the depth of the layer.

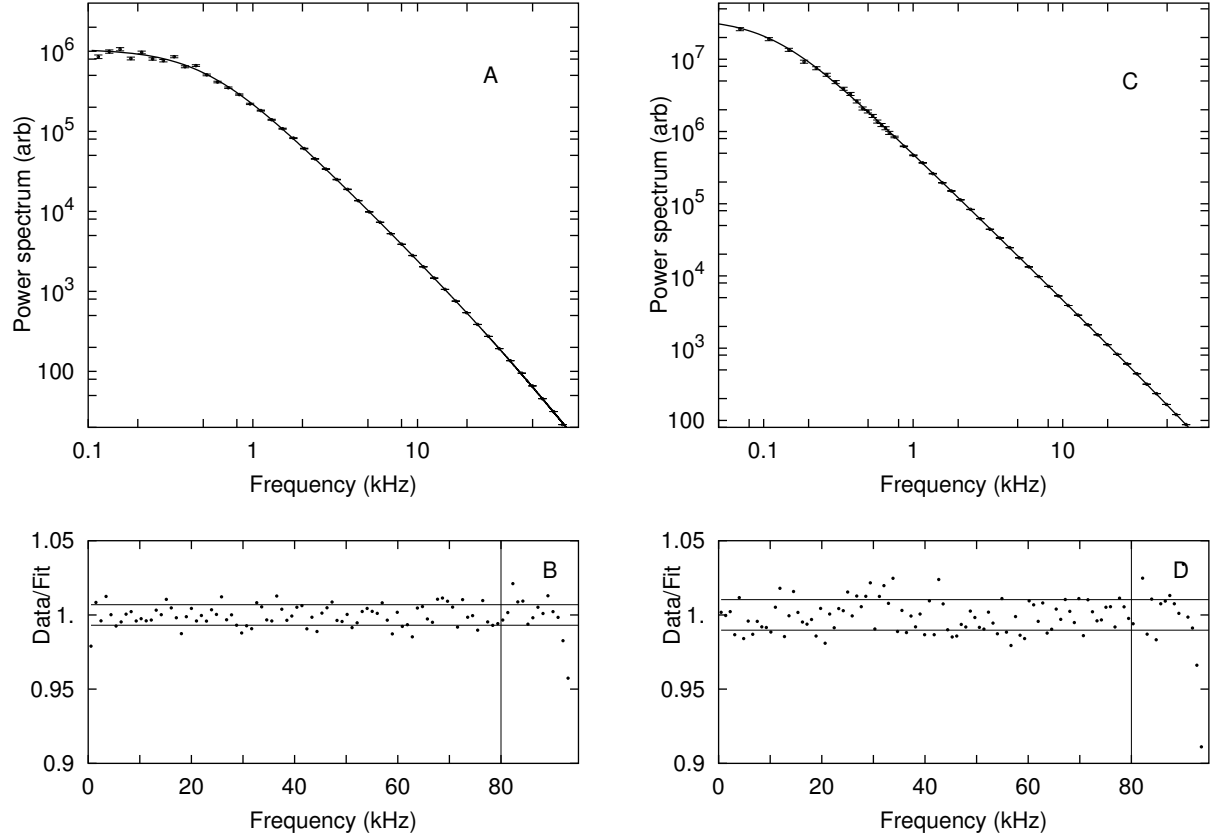


Figure 4. Calibration fits for two different photo diodes. Panels A and B: data set obtained with tuneable laser at a wavelength of 950 nm, recorded by Si-PIN photodiode. Panels C and D: data set obtained with 1064 nm laser, recorded by InGaAs diode. Panels A and C show the power spectra in log-log plots. Data are shown with error bars, barely visible to the eye at high frequencies. Solid lines show fits of $G(f)P_{\text{hydro}}(f)$ to the data. For the data set recorded by the Si-PIN diode, the two slowest eigenmodes of diffusion were included, e.g., $N=1$ in Eq. (6). For the data set recorded by the InGaAs diode, only one mode was included, $N = 0$. Panels B and D show residual plots of data divided by fit, with the theoretical standard deviation shown as two horizontal lines. The vertical line at 80 kHz indicate the upper frequency cut-off in data fitted to. This cut-off was chosen because an electronic filter in the data acquisition system causes a sharp cut-off near 90 kHz, with some ripples (not visible here) just below 90 kHz. Table 1 shows parameter values for parasitic filters, as determined from fits shown here.

5. CONCLUSIONS

Both experiments discussed above demonstrate parasitic filtering in the Si-PIN photodiode detection system. For wavelengths as low as 800 nm, it is necessary to account for this filtering in order to interpret the experimental power spectrum quantitatively, when the maximum frequency considered exceeds ~ 40 kHz.⁸

We need at most the two slowest modes of charge-carrier diffusion in order to account fully for the phenomenon, quantitatively and to perfection. Thus the cost of doing this is the introduction of the four fitted parameters describing the two slowest modes. At this cost, we have extended the quantitatively interpretable part of the power spectrum obtained with a 1064 nm laser from approximately 1 kHz to the maximum frequency, 80 kHz, permitted by the $\Delta - \Sigma$ data acquisition electronics. For laser wavelength below 925 nm, we needed only the slowest mode of diffusion, hence only two fitting parameters, to describe the parasitic filter.

In Ref. 12, this new extended bandwidth of tweezers is successfully used to study rheological properties of the yeast cytoplasm *in vivo*. In Ref. 13, on the other hand, the covariance is too large between the parameters describing the biological system of interest and the parameters describing the parasitic filter. The simplest experimental protocol, simultaneous fitting of all parameters, is consequently insufficient to extract the information one is after. In Ref. 6, the soundness of this simplest protocol is discussed in some detail for the simple problem of calibrating an optical trap containing a micro-sphere.

In general, rapid photo detection with a photodiode must, before it is used for quantitative purposes, be considered critically with an eye peeled for parasitic filters. In some cases this is done very easily by copying the chopper experiment described above. In general, when the characteristic function given above can account for parasitic filtering, and determination of its parameters does not interfere with the measurements of interest, high precision and high bandwidth can be achieved with optical tweezers.

ACKNOWLEDGMENTS

This work was supported by the Danish Research Councils and the Carlsberg Foundation. Also, support from a VIDI grant from the Research Council for Earth and Life Sciences and grants from the Foundation for Fundamental Research on Matter (FOM), both with financial support from the Netherlands Organization for Scientific Research (NWO) are acknowledged. We thank the Colloid Synthesis Facility, Utrecht University, for kindly providing silica beads.

REFERENCES

1. G. Meyer and N. M. Amer, "Novel optical approach to atomic force microscopy," *Appl. Phys. Lett.* **53**, pp. 1045–1047, 1988.
2. S. Alexander, L. Hellems, O. Marti, J. Schneir, V. Elings, P. K. Hansma, M. Longmire, and J. Gurley, "An atomic-resolution atomic-force microscope implemented using an optical lever," *J. Appl. Phys.* **65**, pp. 164–167, 1989.
3. A. D. Mehta, J. T. Finer, and J. A. Spudich, "Reflections of a lucid dreamer: Optical trap design considerations," *Meth. Cell Biol.* **55**, pp. 47–69, 1998.
4. F. Gittes and C. F. Schmidt, "Interference model for back-focal-plane displacement detection in optical tweezers," *Opt. Lett.* **23**, pp. 7–9, 1998.
5. K. Berg-Sørensen, L. Oddershede, E.-L. Florin, and H. Flyvbjerg, "Unintended filtering in a typical photodiode detection system for optical tweezers," *J. Appl. Phys.* **93**, pp. 3167–3176, 2003.
6. K. Berg-Sørensen and H. Flyvbjerg, "Power spectrum analysis for optical tweezers," *Rev. Sci. Ins.* **75**, pp. 594–612, 2004.
7. E. J. G. Peterman, M. van Dijk, L. C. Kapitein, and C. F. Schmidt, "Extending the bandwidth of optical-tweezers interferometry," *Rev. Sci. Ins.* **74**, pp. 3246–3249, 2003.
8. K. Berg-Sørensen, E. J. G. Peterman, M. van Dijk, C. Schmidt, and H. Flyvbjerg, "Power spectrum analysis for optical tweezers, II: Laser wavelength dependence of parasitic filtering and how to achieve high bandwidth," *submitted*, 2004.

9. F. Gittes, B. Schnurr, P. D. Olmsted, F. C. MacKintosh, and C. F. Schmidt, "Microscopic viscoelasticity: Shear moduli of soft materials determined from thermal fluctuations," *Phys. Rev. Lett.* **79**, pp. 3286–3289, 1997.
10. C. Veigel, M. L. Bartoo, D. C. W. White, J. C. Sparrow, and J. E. Molloy, "The stiffness of rabbit skeletal actomyosin cross-bridges determined with an optical tweezers transducer," *Biophys. J.* **75**, p. 1424, 1998.
11. L. Oddershede, H. Flyvbjerg, and K. Berg-Sørensen, "Single-molecule experiment with optical tweezers: Improved analysis of the diffusion of the λ -receptor in *E.coli*'s outer membrane," *J. Phys.: Condens. Mat.* **15**, pp. S1737–S1746, 2003.
12. I. M. Tolić-Nørrelykke, E.-L. Munteanu, G. Thon, L. Oddershede, and K. Berg-Sørensen, "Anomalous diffusion in living yeast cells," *Phys. Rev. Lett.*; to appear, 2004.
13. K. Berg-Sørensen, L. Oddershede, and H. Flyvbjerg, "Optical tweezers as a tool of precision: Single-molecule mobility as case study," *Proceedings of SPIE, Photonics West 2004*, 2004.
14. N. W. Ashcroft and N. D. Mermin, *Solid State Physics*, Saunder's College, Philadelphia, PA, Holt-Saunders Int'l. ed., 1981.
15. "Photodiodes (hamamatsu)." Cat. No. KPD0001E07, 1998.
16. "Photodiode Characteristics, UDT Sensors Inc.," 2002. www.udt.com.
17. W. H. Press, B. P. Flannery, S. A. Teukolsky, and W. T. Vetterling, *Numerical Recipes*, Cambridge University Press, 1986.
18. M. W. Allersma, F. Gittes, M. J. deCastro, R. J. Stewart, and C. F. Schmidt, "Two-dimensional tracking of ncd motility by back focal plane interferometry," *Biophys. J.* **74**, pp. 1074–1085, 1998.
19. R. Kubo, M. Toda, and N. Hashitsume, *Statistical Physics*, vol. 2, Springer-Verlag, Heidelberg, 1985.
20. H. Flyvbjerg *unpublished*, 2003.
21. K. Berg-Sørensen and H. Flyvbjerg, "Erratum to: Power spectrum analysis for optical tweezers," *Rev. Sci. Ins.* **75**, pp. 594–612, 2004.